

Engineering of Band Gap in Metal–Organic Frameworks by Functionalizing Organic Linker: A Systematic Density Functional Theory Investigation

Hung Q. Pham,^{†,‡,⊥} Toan Mai,[†] and Nguyen-Nguyen Pham-Tran^{*,†,‡}

[†]Faculty of Chemistry, University of Science, Vietnam National University, 227 Nguyen Van Cu, District 5, Ho Chi Minh City, Vietnam

[‡]Institute for Computational Science and Technology, SBI Building, Quang Trung Software City, Tan Chanh Hiep Ward, District 12, Ho Chi Minh City, Vietnam

[⊥]Molecular and NanoArchitecture (MANAR) Center, Ho Chi Minh, 721337, Vietnam

Yoshiyuki Kawazoe[§] and Hiroshi Mizuseki[§]

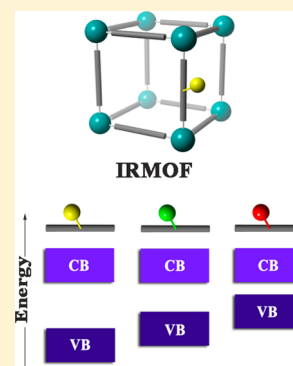
[§]Institute for Materials Research, Tohoku University, 2-1-1 Katahira, Aoba-ku, Sendai, Miyagi, 980-8577, Japan

Duc Nguyen-Manh^{||}

^{||}Theory and Modeling Department, Culham Centre for Fusion Energy, United Kingdom Atomic Energy Authority, Abingdon, OX14 3DB, United Kingdom

S Supporting Information

ABSTRACT: A systematic investigation on electronic band structure of a series of isorecticular metal–organic frameworks (IRMOFs) using density functional theory has been carried out. Our results show that halogen atoms can be used as functional groups to tune not only the band gap but also the valence band maximum (VBM) in MOFs. Among halogen atoms (F, Cl, Br, I), iodine is the best candidate to reduce the band gap and increase the VBM value. In addition, it has been found that for the antiaromatic linker DHPDC (1,4-dihydropentalene-2,5-dicarboxylic acid) the energy gap is 0.95 eV, which is even lower than those calculated for other aromatic linkers, i.e., FFDC (furo[3,2-b]furan-2,5-dicarboxylic acid) and TTDC (thieno[3,2-b]thiophene-2,5-dicarboxylic acid). By analyzing the lowest unoccupied molecular orbital–highest occupied molecular orbital gaps calculated at the molecular level, we have highlighted the important role of the corresponding organic linkers in the MOF band gap. In particular, the change of C–C–C=O dihedral angle in the organic linker can be used to analyze the difference of band gaps in MOF crystals. It is shown that a deep understanding of chemical bonding within linker molecules from electronic structure calculations plays a crucial role in designing semiconductor properties of MOF materials for engineering applications.



I. INTRODUCTION

Over the past few decades metal–organic frameworks (MOFs)^{1,2} have been recognized as a new class of porous crystalline materials which are promising for diverse applications, such as gas storage and separation,^{3–5} catalysis,⁶ chemical sensors,⁷ and drug delivery.⁸ Furthermore, MOFs have also attracted a great deal of attention because of their structural and chemical diversity. This characteristic was explained by their inorganic–organic hybrid nature. The varying of these components created more than 20 000 MOFs⁹ which are different in many significant properties, including porosity, internal surface area, pore aperture or diameter, and functional group.^{10–12}

The reticular chemistry¹³ suggests that it is possible to predetermine the property of MOF materials via rationalizing the design of linkers. This requires a good understanding about the relationship between chemical bonding and structural properties of the material. Together with experiments, molecular modeling are powerful tools for providing fundamental knowledge for designing new materials with desirable properties. Frost and Snurr¹⁴ used grand canonical Monte Carlo simulation to establish the requirements of MOFs for hydrogen storage. They concluded that depending on the

Received: June 17, 2013

Revised: February 12, 2014

Published: February 12, 2014

pressure range the amount of absorbed hydrogen will correlate with the corresponding heat of adsorption, surface area, or free volume of material. Recently, by using large-scale screening approach for 137 953 MOFs, Wilmer et al.¹⁵ generated over 300 new potential compounds which have the predicted capacity for methane storage higher than that of any MOF reported so far. Moreover, they have discovered the relationship between the methane-storage capability and the porous properties of the material, i.e., surface area and void fraction. Their prediction was strongly confirmed through the successful synthesis of NOTT-107. Most of the studies on MOF materials have thus far been particular focused on gas storage and selectivity properties; the electronic structures and their applications have received much less systematic investigation.

Among their diverse functionalities and applications,^{16,17} MOFs can be used as promising semiconductor materials because of their “tunability” property.^{18–21} In solid-state chemistry, electronic structure calculations provide a theoretical background for understanding many physical properties in materials, in particular, the electron charge transfer or hybridization states in crystalline system. Determination of band gap plays a crucial role in semiconductor materials, and it would be important to understand the origin of this value for specific applications, e.g., electrical conductivity, photocatalyst, and so forth. In general, the band gap engineering in MOFs materials can be studied by varying either the metallic oxide cluster or functionalizing the organic linker. Lin et al.²² showed that the band gap value can alter by varying the cluster size and the conjugation of the linker. Interestingly, another investigation²³ reported that the semiconductor nature of IRMOF-1 can be changed to metallic behavior via tailoring Zn atoms in $Zn_4O(CO_2)_6$ cluster with Co atoms. So far, there are no experimental works carried out in this direction, possibly because it is quite difficult to form MOFs structures composed from $Co_4O(CO_2)_6$ cluster with organic linkers. Instead, the band gap engineering by linker functionalization is more efficient than the changing of metal strategy because of retrosynthesis²⁴ of organic compound. In addition, Kuc et al.²⁵ studied the band gap of a series of isorecticular structures with IRMOF-1 and revealed the dominant role of organic linkers in electronic structure of these materials. They also found that by altering the conjugation of the linker, the energy gap can be controlled between 1.0 and 5.5 eV within density functional-based tight-binding (DFTB) method. To the best of our knowledge, most of the previous studies on MOF’s semi-conducting band gap focused on the linker conjugation; the effect of functional groups was not really considered until now. In this work, using density functional theory (DFT), we have systematically studied the electronic structure of a series of IRMOFs constructed from twelve linear linkers in order to clarify the following issues.

- (i) What is the effect of different chemical elements (halogens, O, S) on band gap control for IRMOFs with the linkers 2-X-1,4-benzenedicarboxylic acid (BDC-X; X = F, Cl, Br, I), furo[3,2-b]furan-2,5-dicarboxylic acid (FFDC), and thieno[3,2-b]thiophene-2,5-dicarboxylic acid (TTDC)?
- (ii) For a low band gap material, is an aromatic linker better than an antiaromatic one for producing MOF materials with low band gap (FFDC and TTDC linker compared with DHPDC linker)?

- (iii) The dominant role of organic linker in comparison to metallic oxide cluster, and the question: Can we predict the MOF’s electronic structure by investigating the structure of the organic linker?

As it will be shown in Results and Discussion, the predicted band gap value for IRMOF-1 and IRMOF-8 are in good agreement with experimental results reported previously.^{26,27} Furthermore, the gap values predicted for some linear linkers also agree well with those calculated from the periodic model in this work and other previous publications as well.^{22,25,27–29} This good agreement makes us believe that the answers to the above questions will provide the fundamental background for designing potentially new semiconductor materials.

II. COMPUTATIONAL DETAILS

To optimize initial materials we have carried out the DFT calculations with the PBE³⁰ (exchange correlation or XC functional) level of theory under the periodic condition using CRYSTAL09.³¹ A previous study²¹ on electronic structure, chemical bonding, and optical properties of the MOF-5 shows that the DFT-PBE method gave a satisfactory agreement between theoretical and experimental values of band gap. The equilibrium structures was used for studying electronic properties, such as band energy, band edge position, and Mulliken charge. MOFs are a kind of hybrid crystalline material that contain both organic and inorganic components. It is important to choose an appropriate basis set that is sensible for describing electronic structure of organic linkers and for those of metallic components as well. Hence, we used the 6-31G basis function for all nonmetallic atoms, i.e., C, H, O, S, F and Cl. For Zn atoms, we use the 6-31G basis function for the outer part or valence basis and effective pseudopotential ECP28MWB,³² which was considered the quasi-relativistic correction, for the inner part or core basis. For heavy atoms, i.e., Br[−] and I[−], the relativistic correction pseudopotentials developed by Doll and Stoll³³ were used. The force convergence criterion was set to 0.00045 and 0.00030 au for maximum component and root-mean-square (RMS) of the gradient, respectively. For self-consistent total energy calculations, the condition was set to 10^{-7} Hartrees during the geometry optimization step. The shrinking factor of reciprocal lattice vectors according to the Pack–Monkhorst method were set to 3, corresponding to 4 k-points at which the Hamiltonian matrix was diagonalized.

For the linker, optimized molecular structure and electronic property were also calculated using Gaussian09³⁴ at the same level as that used for the periodic system to maintain consistency. As discussed in the following section, within our systematic investigation of IRMOF crystals with different chemical elements for the linker molecules, the conventional space group symmetry $Fm\bar{3}m$ will be replaced by a lower simple cubic crystal symmetry $Pa\bar{3}$. The latter has the main advantage of optimizing different degrees of freedom when performing electronic structure calculations of linker molecules using Gaussian code. In Supporting Information, we have provided Figure S1 (and Table S10) illustrating the degree of freedom for Br atom in the IRMOF-2Br crystal as well as Figure S2 (and Table S12) for the H1 and H2 atoms in the IRMOF-20S crystal within the same $Pa\bar{3}$ space group. The 6-311++G(d,p) basis set was used for all atoms. By using the same functional for exchange correlation energy in both cases, the discrepancy due to the basis set differences between two different codes was

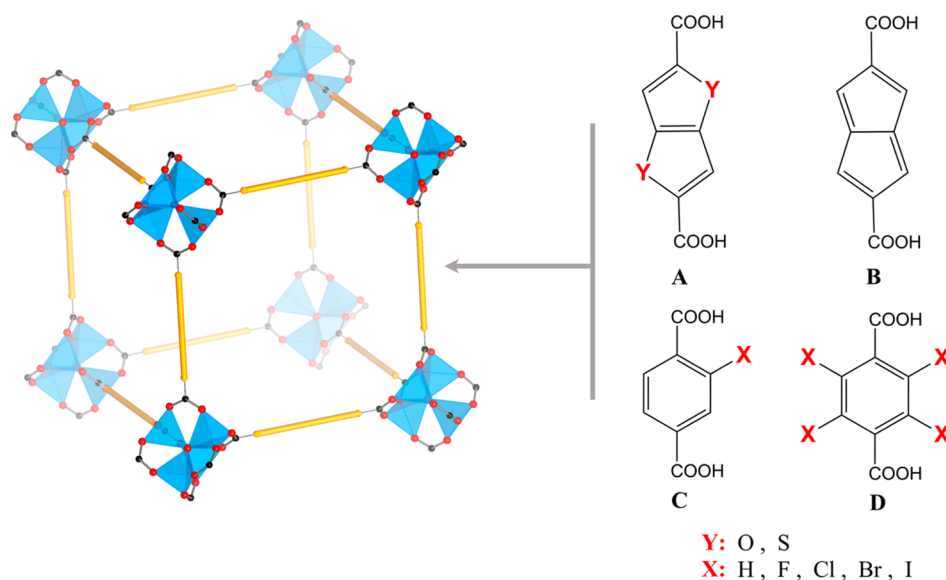


Figure 1. Left panel: isorecticular pcu-MOF model. Orange cylinders are organic linkers (A, B, C, and D), and blue polyhedra are metallic oxide clusters ($\text{Zn}_4\text{O}(\text{CO}_2)_6$). Right panel: 12 organic linkers investigated in this work. FFDC (linker A with Y = O), TTDC (linker A with Y = S), DHPDC (linker B), BDC-X (linker C with X = H, F, Cl, Br, I), and BDC- X_4 (linker D with X = H, F, Cl, Br, I).

negligible. This approach comparing electronic structure calculations of linker molecules between free configurations and inside crystals proves to be useful for understanding band gap properties in different MOF materials.

III. RESULTS AND DISCUSSION

Structural Details. In this work, we have carried out a systematic study to design eight isorecticular MOFs (IRMOFs)¹¹ with different kinds of linear linkers (as shown in Figure 1), namely, IRMOF-20C (DHPDC), IRMOF-20O (FFDC), IRMOF-20S (TTDC), IRMOF-2X (BDC-X; X = F, Cl, Br, I), and IRMOF- F_4 . Among these structures, IRMOF-20 and IRMOF-2X materials were experimentally synthesized;^{35,36} others were just the hypothetical MOFs, i.e., IRMOF-20C, IRMOF-20O, and IRMOF- F_4 . In addition, a well-known compound IRMOF-1 (or MOF-5)³⁷ was also included in this study because it is considered to be the metal–organic framework reference material for comparison with other compounds.

IRMOFs were made by assembly of Zn_4O cluster and linear dicarboxylic linkers. These components play roles similar to nodes and struts to create a cubic framework with topology pcu-a (cab). When the linker is replaced and the metallic oxide cluster is kept, new MOFs can be created without changing the underlying topology. Constructing a crystal unit cell for quantum calculation requires a well-defined material symmetry or space group, especially for extended crystals which can contain hundreds of atoms per unit cell. From experiments,¹¹ the conventional space group of IRMOFs is the face-centered cubic (FCC) space group: $Fm\bar{3}m$. However, in the presence of low symmetric linkers, this space group cannot be used for describing well our structures, for instance, IRMOF-20. For this reason, we used $Pa\bar{3}$ instead of the $Fm\bar{3}m$ space group for constructing most structures (the exceptions were IRMOF-1 and IRMOF- F_4).

The calculated structural parameters for all structures are shown in Table 1. The averaged bond and angle values for IRMOF-1, IRMOF-2, and IRMOF-20 are in a good agreement with experimental data presented in Tables S10–S12 in the

Table 1. Optimized Crystal Structure Lattice Parameters

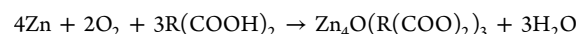
	symmetry	atoms/ cell	<i>a</i> (Å)	ΔH_f (kcal/mol)
IRMOF-2F	$Pa\bar{3}$	424	26.2001	−691
IRMOF-2Cl	$Pa\bar{3}$	424	26.2091	−692
IRMOF-2Br	$Pa\bar{3}$	424	26.2040 (25.7718 ^a)	−692
IRMOF-2I	$Pa\bar{3}$	424	26.1917	−693
IRMOF-20C	$Pa\bar{3}$	472	29.1516	−692
IRMOF-20O	$Pa\bar{3}$	424	28.7546	−695
IRMOF-20S	$Pa\bar{3}$	424	29.7161 (29.1840 ^b)	−697
IRMOF- F_4	$Fm\bar{3}m$	424	26.3502	−689
IRMOF-1	$Fm\bar{3}m$	424	26.1595 (25.6690 ^c)	−691

^aExperimental data from ref 11. ^bExperimental data from ref 36.

^cExperimental data from ref 37.

Supporting Information. The unit cell parameter (*a* value) of IRMOF-2X (X = F, Cl, Br, I) series is not significantly different. For the hypothetical structures IRMOF-20C, IRMOF-20O, and IRMOF- F_4 , it would be good to have structural data from experimental measurements for validating our theoretical prediction.

The enthalpy of formation is a well-known quantity to determine the stability of any hypothetical compound. A negative value of enthalpy of formation would suggest that the considered structure can be thermodynamically stable and possibly synthesized experimentally. In this work, the enthalpies of formation were calculated from the difference between the total energy between the products and reactants according to the following reaction:



The total energies of the gas phase of Zn, O_2 , H_2O , and linker $\text{R}(\text{COOH})_2$ were computed using the same basis set as that used for the $\text{Zn}_4\text{O}(\text{R}(\text{COO})_2)_3$ crystalline phase. The enthalpies of formation data are shown in Table 1. The strongly negative values of formation energy have confirmed the stability

Table 2. Band Energy Values (in Electronvolts) Calculated from Periodic Systems and Linker Molecules

	VBM position ^a	CBM position ^a	E_g^a	E_{HOMO}^b	E_{LUMO}^b	$E_{\text{LUMO}} - E_{\text{HOMO}}^b$
IRMOF-2F	-6.49	-3.29	3.20	-6.90	-3.45	3.45
IRMOF-2Cl	-6.44	-3.35	3.09	-6.72	-3.46	3.26
IRMOF-2Br	-6.29	-3.33	2.96	-6.58	-3.46	3.11
IRMOF-2I	-5.96	-3.31	2.65	-6.35	-3.59	2.76
IRMOF-20C	-5.19	-4.24	0.95	-5.69	-4.66	1.03
IRMOF-20O	-5.59	-2.94	2.65	-6.20	-3.39	2.80
IRMOF-20S	-5.90	-3.38	2.52	-6.19	-3.44	2.75
IRMOF-F ₄	-6.39	-3.62	2.77	-6.76	-3.84	3.34
IRMOF-1	-6.59	-3.13	3.46	-6.86	-3.30	3.56

^aCalculated from crystalline systems. ^bCalculated from linker molecules.

of the studied compounds. Additionally, the formation energies of IRMOF-2X (X = F, Cl, Br, I) which are in the range of -691 to -694 kcal/mol are comparable with that of IRMOF-1 (-691 kcal/mol). It should be noted that these results are entirely consistent with successful synthesis of these MOFs. The replacing of TTDC linker by DHPDC makes the formation energy increase by 5 kcal/mol as compared that of IRMOF-20 (-697 kcal/mol); the structure became less stable than the original. This compound is, however, still stable if compared to IRMOF-1; thus, it would be possible to produce it by experiment.

Electronic Structure Calculation for Periodic Systems.

The electronic band structure calculations have been performed in the first Brillouin zone by specifying a set of coordinates of high symmetric points. The path in the reciprocal space is Γ -X-L-W- Γ for $Fm\bar{3}m$ space group and Γ -R-M-X- Γ for $Pa\bar{3}$. Band gap value has been determined by the energy difference between the valence band maximum (VBM) and the conduction band minimum (CBM) at Γ (gamma) point. Conventionally, DFT methods underestimate band gap in comparison with experimental value.³⁸ Bartolomeo et al.³¹ reported the energy gap for MOF-5 (or IRMOF-1) is 5.0 eV by using DFT-B3LYP method, which is significantly higher than the experimental value of 3.4 eV.²⁶ In other works, by using the generalized gradient approximation Perdew-Burke-Ernzerhof (GGA-PBE)³⁰ functional for XC energy, the calculated energy gap for MOF-5 is 3.5 eV,²¹ which is in an excellent agreement with experiment. The GGA-PBE level of theory also gave reasonable results for other MOFs, such as IRMOF-8,²⁷ IRMOF-10,²⁸ and IRMOF-14²⁹ even though there are no experimental values for some materials. Therefore, the present DFT calculations shown in Table 2 confirmed the results from previous studies¹⁶ that the GGA-PBE functional unexpectedly gave a band gap value in a good agreement with the existing experimental data. Different functionals were used to investigate the effect of XC functional on band gap, and the result is given in Table S13 of the Supporting Information). Our result showed that Hartree-Fock eigenvalue is clearly not a good approximation for studying the electronic band structure of the MOF-5 crystal system. The predicted band gap value from Hartree-Fock calculation is 8.43 eV, which is overestimated in comparison with the experimental value of 3.4 eV. Additionally, varying the Fock exchange percentage in the hybrid DFT method also alters the predicted band gap. The higher the percentage of HF contribution, the higher the value of the band gap. The B3LYP, a hybrid functional with percentage up to 20%, gave the gap value higher than experiment. This result is completely consistent with previous work.³¹ From Table S13 (in the Supporting Information), it is

clear that among studied methods, the GGA-PBE functional predicted the most sensible result in comparison to the others. In our calculations, the GGA-PBE functional was used for investigating electronic structure because of the two following reasons: (1) GGA tends to improve many kinds of electronic properties, such as total energy, atomization energies, energy barriers, and structural energy differences by including the effects of local gradients in the charge density in comparison with the local density approximation (LDA).³⁹ (2) The band gap energy calculated for MOF-5 using DFT-PBE is in good agreement with experimental and other theoretical studies.

Our electronic structure calculations show that the positions of maximum valence band energy and minimum conduction band energy for the all considered MOF structures are located at the same Γ k-point (see Figures S1-S9 from the Supporting Information). Consequently, the k-vectors for VBM and CBM are the same, and we conclude that within our studies the IRMOF's band gap is a direct one. For illustration, band structure of IRMOF-2F ($Pa\bar{3}$ symmetry) and IRMOF-F₄ ($Fm\bar{3}m$ symmetry) are shown in Figure 2. The band structure of other MOFs can be found in the Supporting Information.

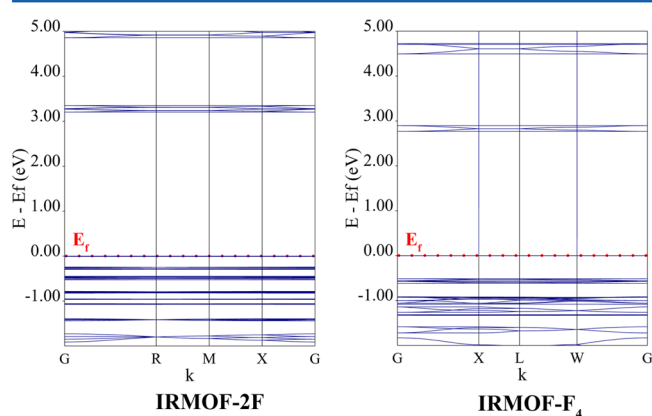


Figure 2. Electronic band structure of IRMOF-2F (left panel) and IRMOF-F₄ (right panel) with space group symmetry $Pa\bar{3}$ and $Fm\bar{3}m$, respectively. The Fermi energy is located at 0 eV.

Figure 3a shows the band edge position at Γ point of IRMOF-2X (X = F, Cl, Br, I) series. The predicted values of semiconductor band gaps in these materials varied from 2.65 to 3.20 eV, which are lower than that obtained for the IRMOF-1 crystal 3.37 eV (in the present study). Hence, introduction of halogen atoms into the aromatic ring can be a cause of reduction in band gap. Interestingly, the energy gap systematically decreases when the atomic size of the halogen atom

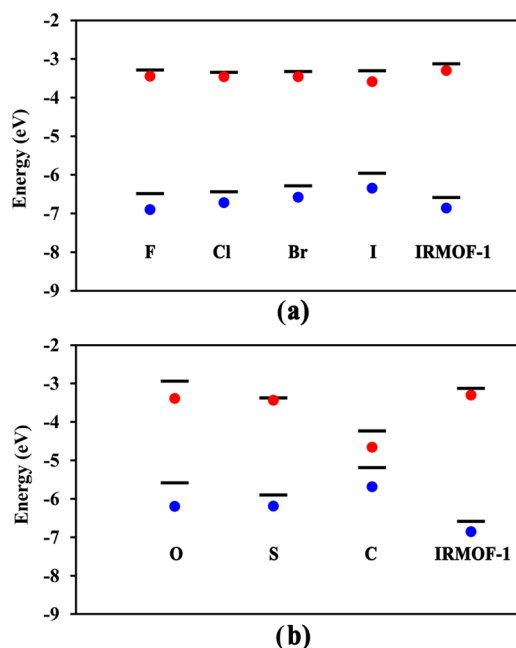


Figure 3. Band edge position of MOFs (Black segment) calculated from electronic band structure of crystalline systems and HOMO–LUMO energy levels obtained from linker molecules (HOMO, filled blue circle; LUMO, filled red circle) for (a) IRMOF-2X and (b) IRMOF-20Y.

increases from F to I. This variation comes from a significant increase of VBM because the difference in CBMs is negligible. The partial density of states (PDOS) are useful to understand this systematic trend. Figure 4 shows the PDOS of s-states and p-states of halogen atoms, BDC part, Zn atom, Zn_4O cluster and the total DOS for IRMOF-2X and IRMOF-20Y. The PDOS pattern shows that obviously the BDC fragment plays an important role in the total density of states (TDOS). The characteristic peaks of this one and those of the TDOS are very similar. Although the orbitals of the Zn_4O cluster also contribute to valence and conduction bands, they are not contributing to the energy region close to the band edge position (VBM or CBM). This suggests that the origin of band gap of Zn_4O -based IRMOFs comes from the organic linker rather than from the metallic cluster. This present result agrees well with the discussion from a previous paper²⁸ as well as the conclusion from the analysis of HOMO–LUMO (the highest occupied and lowest unoccupied molecular orbital, respectively) data in the following section. Figure 4 also shows that the p-orbitals of the halogen atom contribute mainly to the region of electronic density of states in the energy region below the Fermi energy, i.e., valence band, whereas the contributions from Zn atoms are dominated in the conduction band. This explains why the halogen basically altered the position of the VBM.

The application of MOFs as an electrical conductor is possible because of the charge transport through a delocalization of electronic states nearby band gap energies. This required a hybridization between the p orbitals in the linker and the metal d orbital.¹⁸ As is shown in Figure 4, the d orbitals of Zn atoms have a dominant contribution in the antibonding conduction band but not in the valence band. This is also consistent with the electronically excited state investigation on MOF-5 reported previously.⁴⁰

To further understand the systematic decrease of energy gap presented in Figure 3a, it is necessary to study carefully the electron distribution in the crystalline system by analyzing the Mulliken charge (Table S14 in the Supporting Information). When the halogen atom is altered, the charge of each atom of the linker is varied. In particular, this variation was more remarkable for the atoms that are in a nearest neighbor coordination with the halogen atom. Going systematically along the series of halogen atom from F to I, the total charge value for the Zn_4O cluster slightly increased (+3.365 to +3.427), and this alteration is negligible in comparison with IRMOF-1 (+3.355). Meanwhile, the total charge value for the BDC part slightly decreased from Cl to I (−1.917, −1.94, −1.993, respectively), but there is a significant decrease in F (−1.467). In contrast, the charge of the halogen atom systematically increases from F (0.345) to Cl (0.789), Br (0.805), and I (0.852). In a comparison with the IRMOF-1 compound, the total charge value of the BDC part is a bit lower for IRMOF-2X except for the case of IRMOF-2F. These calculations showed that there is essentially a charge transfer from Cl, Br, and I atoms to the benzene ring, whereas the opposite direction of charge transfer has been observed for F, which has the highest electronegativity among halogen atoms. We note that the VBM position of IRMOF-2X increased systematically, and it was less sensitive to the direction of electron charge transfer mentioned previously. It is well-known that the substituent effect of the halogen group in the aromatic ring can be considered an electron-withdrawing group by −I effect (inductive effect) or an electron-releasing group by +C effects (conjugated effect).⁴¹ In this case, the contribution of the p-state of the halogen atom to conjugated system is dominant and thus leads to the increase of HOMO energy position by pushing electrons toward the aromatic ring. Furthermore, this effect is reinforced by the electronegativity trend reducing from F to I. In summary, the altering of the halogen atom from F to I can reduce the energy band gap via raising the HOMO energy.

Figure 3b shows the band edge position of the series of IRMOF-20Y crystal in which O atom is replaced by S and C atoms. Similar to the effect of a halogen, the replacement of the O atom, a high electronegative element, by the S atom reduced the energy gap from 2.65 to 2.52 eV. Unlike IRMOF-2X, both the VBM and CBM positions in IRMOF-20Y decreased with the change of chemical substitutions; this can be further confirmed by analyzing the contribution of s-states and p-states of X atoms in the total DOS (Figure 5). Interestingly, we have found that the gap value is reduced to 0.95 eV when the aromatic linker changed to DHPDC, an antiaromatic linker⁴² (Figure 6). This latter value approximated the band gap of silicon, a common semiconductor in industrial electronic devices, which is about 1.17 eV. However, DHPDC is perhaps unstable because of the high HOMO energy compared to those in FFDC and TTDC. This finding is in agreement with the trend of formation energy data discussed in the previous section. In our opinion, a promising linker must be highly thermodynamically stable in addition to its ability to reduce band gap of MOFs. Therefore, tuning the band gap by altering the electronic structure of the organic linker is more efficient than functionalizing the conjugated system by donor and acceptor groups.

The above analysis from complex crystalline structures has provided a useful insight into the electronic structures of MOF compounds. In the next subsection we show that the origin of

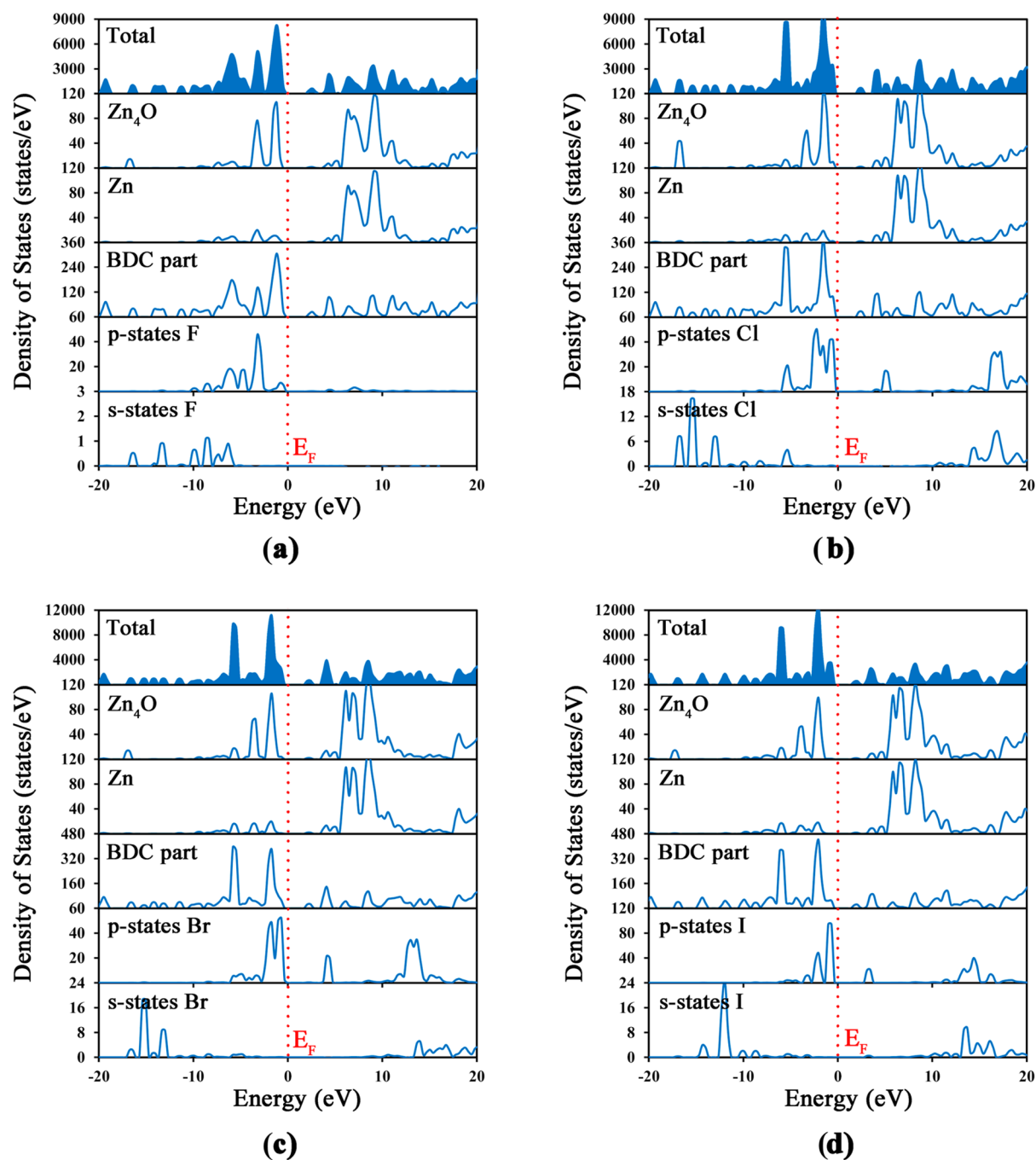


Figure 4. The total density of states (TDOS) and partial density of states (PDOS) for IRMOF-2X: (a) IRMOF-2F; (b) IRMOF-2Cl; (c) IRMOF-2Br; (d) IRMOF-2I. The dotted red line is the Fermi level.

the band gap can be understood from first-principles calculations of the corresponding linker clusters.

HOMO–LUMO Gap from Linker. We now return to the interesting question mentioned in the Introduction, namely, can we predict band gap energies of MOF compounds by investigating the electronic structure of their organic linkers? To answer this question, the energy gaps from the HOMO–LUMO of the linker were calculated and are denoted by filled red and blue circles in Figure 3. It is necessary to note that through the geometry optimization the dihedral angle between two carboxylic groups of linkers was constrained at zero value to keep this structure similar to the linker configuration in the

crystal. We found that although the exact values of band edge positions are not the same in the two cases, the trend of HOMO–LUMO is in amazing agreement with those of the corresponding band gap energies calculated in the previous section for all the crystal systems. In addition, the difference between the energy gap estimated from the linker and from the crystalline phase is relatively small (less than 0.25 eV). Obviously, the topological structure containing the metal element contributes to this small difference in band gap energies. Regarding the effect of the metal, Yang and co-workers^{28,29} reported the properties of IRMOFs based on two linkers, HPDC (4,5,9,10-tetrahydropyrene-2,7-dicarboxylate)

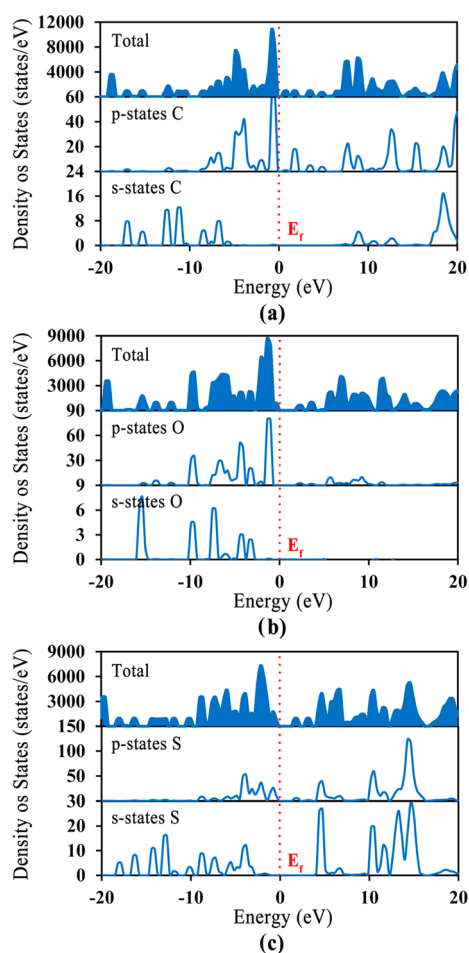


Figure 5. The total density of states (TDOS) and p-states density of states (PDOS) for IRMOF-20Y: (a) IRMOF-20C; (b) IRMOF-20O; (c) IRMOF-20S. The dotted red line is Fermi level.

and PDC (pyridine-3,5-dicarboxylate), and different kinds of metal elements, namely, Zn, Cd, Be, Mg, Ca, Sr, and Ba. Their result shows that the band gap variation by changing the metal is negligible in comparison with the effect of the linker. In other work,²⁵ the replacement of Zn atoms in IRMOF-1 by Co atoms can tune the electronic structure from semiconducting to metallic state. To the best of our knowledge, the $Zn_4O(CO_2)_6$ cluster is the most popular structure among many octahedral

secondary building units (SBUs).⁴³ Although it is possible to experimentally realize $M_4O(CO_2)_6$ clusters ($M = Co, Be$),^{44,45} so far MOFs based on these clusters have not been reported. Moreover, the chemical structures of organic linkers are not only more diverse than those of the metallic oxide cluster but also more straightforward to control because of the power of retrosynthesis. Hence, metal substitution for tuning the band gap is less favorable than the linker substitution. Crystal net control through the rational design of the geometric structure of the linker has also been reported.^{13,46} Herein, we show that it is possible to engineer the band gap of the material by the rational design of the chemical structure of the linker. The agreement between the band gap energy calculated from MOF crystal structures with those obtained from the HOMO–LUMO energy of the corresponding linker opens an efficient strategy for screening promising linkers for semiconductor applications. In this paper, the HOMO–LUMO gap is used to imply the energy value calculated from the linker cluster, whereas the band gap energy is the terminology used for those values calculated from the periodic system.

In the discussion above, we showed that the halogen atoms as a substitute group in benzene ring can reduce the energy gap by increasing the HOMO energy. This raises an important question: Can the increase of the number of halogen atoms further reduce the band gap? Figure 7 shows the gap estimated

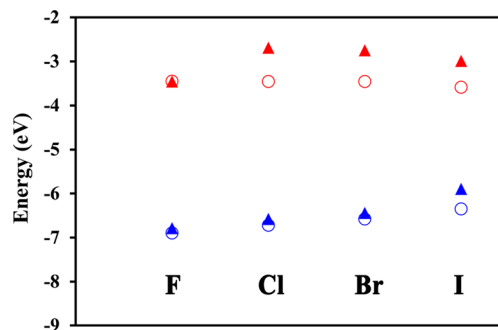


Figure 7. HOMO–LUMO energies calculated for BDC- X_4 linker (HOMO, solid blue triangles; LUMO, solid red triangle) and BDC- X linker (HOMO, open blue circle; LUMO, open red circle).

from HOMO–LUMO energy of linker BDC- X and BDC- X_4 ($X = F, Cl, Br, I$). In the case of BDC- F_4 linker, its estimated energy gap is 3.34 eV, which is lower than the value of BDC- F

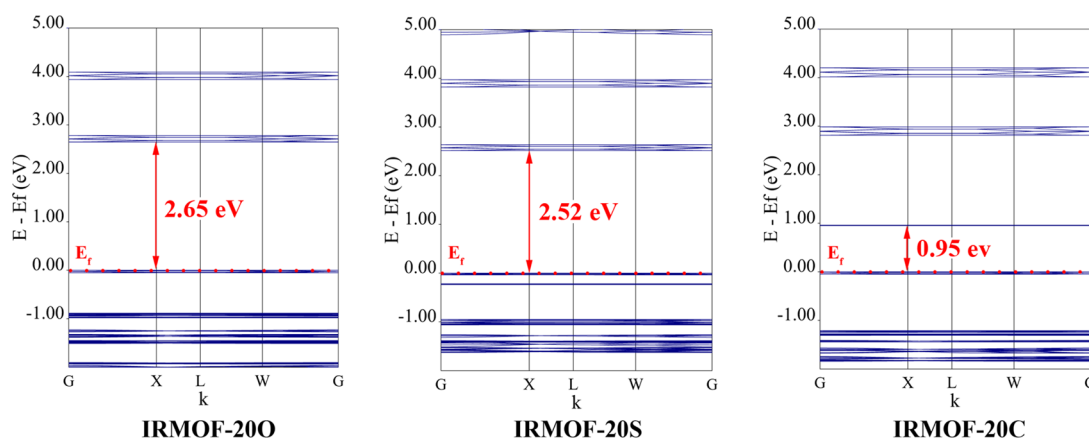


Figure 6. Electronic band structure for IRMOF-20Y: IRMOF-20C, IRMOF-20O, and IRMOF-20S. The Fermi energy is located at 0 eV.

Table 3. Band Gap Estimated from HOMO–LUMO Energy (in Electronvolts) of Linker BDC- X_4 ($X = F, Cl, Br, I$)

linker	dihedral angle ($C_{Ar}-C_{Ar}-C=O$) (deg)	E_{HOMO}	E_{LUMO}	$E_{LUMO} - E_{HOMO}$	linker BDC-X
BDC- F_4	46	-6.79	-3.46	3.34	3.45
BDC- F_4	0	-6.76	-3.84	2.92	
BDC- Cl_4	90	-6.58	-2.69	3.90	3.26
BDC- Br_4	90	-6.44	-2.75	3.69	3.11
BDC- I_4	90	-5.90	-2.99	2.91	2.76

(3.45 eV). We note, however, that the obtained HOMO–LUMO value is much higher than those calculated from crystalline system of IRMOF- F_4 (2.77 eV). The difference between $C_{Ar}-C_{Ar}-C=O$ dihedral angle in the two systems can be the origin of this discrepancy. Indeed, the dihedral angle value of the linker BDC- F_4 is 46° , obtained from fully relaxed calculations, in comparison with 0° constrained by the symmetry of the crystalline system (as indicated in Table 3). To understand this constraint, the zero value of the dihedral angle was fixed within the linker optimization. The HOMO–LUMO gap for this configuration (2.92 eV) is in closer agreement with the calculated band gap of IRMOF- F_4 (2.77 eV). However, harmonic vibrational frequencies calculated for this constrained dihedral angle configuration showed that there are two negative frequency modes (-53.13 and -48.03 cm^{-1}); therefore, this constrained structure is not a stationary point in the potential energy surface. In the case of other halogens (Cl, Br, and I), the lowest-energy structure is the configuration in which the dihedral angle is 90° (Table 3). Accordingly, the energy gap of BDC- X_4 increased instead of decreased in comparison with that of the BDC-X linker. Figure 8 shows how

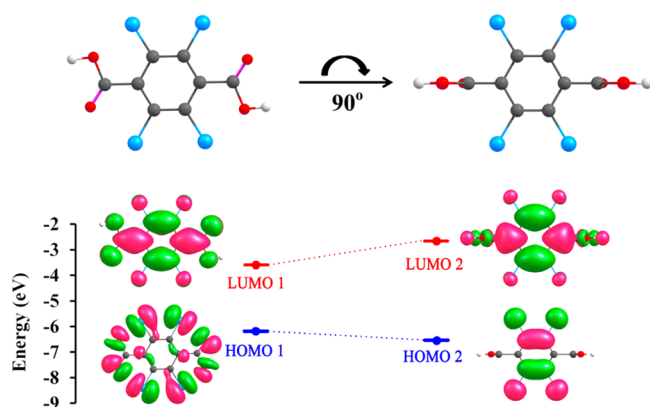


Figure 8. HOMO–LUMO energies of two kinds of conformers of BDC- Cl_4 (left panel, planar conformer; right panel, vertical conformer). Gray, red, blue, and white represent C, O, Cl, and H, respectively.

the HOMO–LUMO energy of the BDC- Cl_4 linker changed by varying the $C_{Ar}-C_{Ar}-C=O$ dihedral angle. When the dihedral angle changed from 0° to 90° , the number of nodes of HOMO–LUMO altered, and this is the cause of the decrease of HOMO energy (the node number decreased) and the increase of LUMO energy (the node number increased). Therefore, the $C_{Ar}-C_{Ar}-C=O$ dihedral angle value can be considered an important factor in predicting the energy gap. Because of the symmetric constraint, the space group $Fm\bar{3}m$ is not appropriate for electronic properties calculation in IRMOF- X_4 ($X = F, Cl, Br, I$). This space group can lead to an unstable configuration because this symmetry requires the $C_{Ar}-C_{Ar}-C=O$ dihedral angle to be zero. Our current work employs the

more flexible space group $Pa\bar{3}$ for almost all materials because this allows the linker to rotate around the axis connecting the carboxylic group with the remaining part of the linker cluster. In summary, the careful consideration of the space group is important for consistency of the periodic calculations in a comparison with the correct prediction of electronic structures from the linker cluster. Linker optimization at the molecular level is also a sensible way to determine the symmetry before implementing on the MOF crystal.

HOMO–LUMO Energy Gap for IRMOFs. Motivated by a strong correlation between electronic structures of linker molecules and the corresponding IRMOF crystals as discussed in HOMO–LUMO Gap from Linker, we now investigate the band gap of some experimental IRMOFs by calculating HOMO–LUMO energy gaps from their linkers (Figure S15 in the Supporting Information). Because there is a lack of measured data on most of the IRMOF crystals, we also use some theoretical values reported in the literature to compare with our data of the corresponding linkers. The predicted HOMO–LUMO energies for all materials are shown in Table 4. In general, most of the investigated IRMOFs showed a

Table 4. Band Gap Estimated from Predicted HOMO–LUMO Energy for Some Experimental IRMOFs

linker	MOF	$E_{LUMO} - E_{HOMO}$ (eV)	E_g (eV)
BDC	IRMOF-1	3.56	3.46 ^a
BDC-Br	IRMOF-2	3.11	2.96 ^a
BDC-NH ₂	IRMOF-3	2.45	
BDC-O-C ₃ H ₇	IRMOF-4	2.57	
BDC-O-C ₈ H ₁₁	IRMOF-5	2.53	
BDC-cycC ₂ H ₄	IRMOF-6	3.31	
BDC-ben	IRMOF-7	2.60	
NDC	IRMOF-8	2.83	3.27/2.91, ²² 2.800 ²⁷
BPDC	IRMOF-10	3.13	2.925, ²⁸ 3.070 ²⁵
HPDC	IRMOF-12	2.81	
PDC	IRMOF-14	2.51	2.454 ²⁹
TPDC	IRMOF-16	2.92	
BDC-(CH ₃) ₄	IRMOF-18	4.00	
TTDC	IRMOF-20	2.75	2.52 ^a

^aThis work.

semiconductor character with an estimated energy gap lower than the 3.56 eV value calculated (this work) for IRMOF-1 crystal. The highest value of 4.0 eV has been obtained for IRMOF-18 because of the rotation of carboxylic group around the C–C axis. This finding is similar to those obtained for the case of IRMOF- X_4 ($X = Cl, Br, I$) shown by blue triangle points in Figure 7. For the derivatives of BDC denoted by the general formula BDC-X-R ($X = N, O$; $R = H, alkyl$), such as BDC-NH₂ (IRMOF-3), BDC-O-C₃H₇ (IRMOF-4), and BDC-O-C₈H₁₁ (IRMOF-5), the HOMO–LUMO energy gaps are significantly lower than those of IRMOF-1. The effect of

releasing electrons from N and O atoms in comparison with C atom would play an important role in this reduction of gap energies. Additionally, the length of alkyl chain almost did not affect the band gap because of the very small difference between the energy gap of IRMOF-4 and IRMOF-5. It is well-known that by the inductive effect (+I) the alkyl group can transfer electrons into the conjugated system as an electron-releasing group. On the basis of the above results, we can conclude that for the band gap reduction the electron donating by the +C effect is more effective than the +I effect. Hence, the electron-donating group by the +C effect is a potential candidate for engineering the band gap of MOFs. One of other ways to alter the energy gap is to control the number of aromatic rings. In fact, band gap decreases when the number of aromatic rings increases. It can be illustrated by the case of either IRMOF-7 (2 rings), IRMOF-8 (2 rings), IRMOF-10 (2 rings), IRMOF-12 (2 rings), IRMOF-14 (4 rings), IRMOF-16 (3 rings) (versus the one-ring system of IRMOF-1), or IRMOF-14 (4 rings), IRMOF-16 (3 rings) (versus the two-ring system of IRMOF-10). The calculated band gap energies of IRMOF-8, IRMOF-10, and IRMOF-14 are confirmed by the studies of Yang and co-workers.^{28,29} In their paper, a DFT optimization for the $Fm\bar{3}m$ crystal system was performed, and band gaps were calculated from DOS patterns. Although their approach is different from ours, their predicted band gaps are surprisingly consistent with the HOMO–LUMO gaps calculated in this work (the errors are within the energy range of 0.03–0.20 eV). This again reinforced our conclusion that the electronic structure of various linkers is the main factor in controlling the semiconductor gap, and it is possible to design a potential MOF by the rational design of organic linkers.

IV. CONCLUSIONS

In our work, the chemical nature of the semiconductor gap of IRMOFs was systematically investigated using first-principles DFT calculations to establish their electronic and structural relationships. Within the present approach, we assume that the effect of the lattice parameter between metallic clusters is negligible and focus on the study of band gap value with fixed framework topology and linker lengths. Consequently, the tunability of band gap depends essentially on the chemical bonding of the organic linker. Our result showed that halogen atoms can be used as a functional group to vary band gap and VBM position in MOFs. Among halogen atoms (F, Cl, Br, I), iodine is the best candidate for reducing the energy gap and increasing the VBM position. We found that replacing O in the FFDC linker by S can also lead to the reduction of band gap energies. However, unlike the effect of halogens, this change involves the reduction of both VBM and CVM in electronic structure; a possible explanation for this effect is the direct contribution of p-orbitals of the O or S atom in the aromatic system. One other interesting result is that the antiaromatic linker DHPDC can reduce significantly the energy gap in comparison to other aromatic linkers, i.e., FFDC and TTDC. The present gap-engineering strategy is even more efficient than the gap variation by simply changing the gap by substituting different elements. This work also showed the dominant role of the organic linker in electronic structures of Zn_4O -based IRMOFs using quantum calculations on both crystal and linker molecules. Henceforth, the MOF electronic band structure can be studied by first-principle calculations on organic linkers instead of performing complicated and time-consuming calculations on the periodic system. Finally, we

would like to point out that for IRMOF-1 the value of CBM position has been found to be -3.13 eV in this study, whereas the experimental value is reported to be -4.7 eV.²⁶ Therefore, more realistic calculations of the electronic band edge positions in aqueous environment⁴⁷ are needed to have a full understanding of this material for the application in solar energy conversion devices.

In summary, the present investigation contributed to the understanding of the chemical effect of organic linkers on the electronic band structure of metal–organic frameworks. The results of this work also established some basic rules for designing new organic linkers for semiconductor applications. Here we are mainly interested in the cubic framework based on the Zn_4O unit which was one of the most popular structures in MOF chemistry. In other words, we have not yet considered the topological diversity of this potential material. Hence, it is important for future work to carry out a large-scale screening using DFT calculation on many other kinds of topology to establish the property–structure relationship in MOF electronic band structure.

■ ASSOCIATED CONTENT

📄 Supporting Information

Details of the fractional atomic coordinates, electronic band structures, and Mulliken charges for nine IRMOFs. This material is available free of charge via the Internet at <http://pubs.acs.org>.

■ AUTHOR INFORMATION

Corresponding Author

*Faculty of Chemistry, University of Science, Vietnam National University, 227 Nguyen Van Cu, District 5, Ho Chi Minh City, Vietnam. E-mail: ptnnguyen@hcmus.edu.vn. Phone: (+84) 905.663.369.

Present Address

Faculty of Chemistry, University of Science, Vietnam National University, 227 Nguyen Van Cu, District 5, Ho Chi Minh City, Vietnam.

Notes

The authors declare no competing financial interest.

■ ACKNOWLEDGMENTS

The authors thank the Institute for Computational Science and Technology (ICST), Ho Chi Minh City for financial support of this project. We acknowledge supercomputing assistance from the Institute for Materials Research at Tohoku University, Japan.

■ ABBREVIATIONS

FFDC, furo[3,2-b]furan-2,5-dicarboxylic acid; TTDC, thieno[3,2-b]thiophene-2,5-dicarboxylic acid; DHPDC, 1,4-dihydropentalene-2,5-dicarboxylic acid; BDC, 1,4-benzenedicarboxylic acid; BDC-X, 2-X-1,4-benzenedicarboxylic acid

■ REFERENCES

- (1) Rowsell, J. L. C.; Yaghi, O. M. Metal–Organic Frameworks: A New Class of Porous Materials. *Microporous Mesoporous Mater.* **2004**, *73*, 3–14.
- (2) Zhou, H.-C.; Long, J. R.; Yaghi, O. M. Introduction to Metal–Organic Frameworks. *Chem. Rev.* **2012**, *112*, 673–674.
- (3) Li, J.-R.; Sculley, J.; Zhou, H.-C. Metal–Organic Frameworks for Separations. *Chem. Rev.* **2012**, *112*, 869–932.

- (4) Murray, L. J.; Dinca, M.; Long, J. R. Hydrogen Storage in Metal-Organic Frameworks. *Chem. Soc. Rev.* **2009**, *38*, 1294–1314.
- (5) Suh, M. P.; Park, H. J.; Prasad, T. K.; Lim, D.-W. Hydrogen Storage in Metal–Organic Frameworks. *Chem. Rev.* **2012**, *112*, 782–835.
- (6) Lee, J.; Farha, O. K.; Roberts, J.; Scheidt, K. A.; Nguyen, S. T.; Hupp, J. T. Metal-Organic Framework Materials as Catalysts. *Chem. Soc. Rev.* **2009**, *38*, 1450–1459.
- (7) Kreno, L. E.; Leong, K.; Farha, O. K.; Allendorf, M.; Van Duyne, R. P.; Hupp, J. T. Metal–Organic Framework Materials as Chemical Sensors. *Chem. Rev.* **2012**, *112*, 1105–1125.
- (8) Horcajada, P.; Chalati, T.; Serre, C.; Gillet, B.; Sebrie, C.; Baati, T.; Eubank, J. F.; Heurtaux, D.; Clayette, P.; Kreuz, C.; et al. Porous Metal-Organic-Framework Nanoscale Carriers as a Potential Platform for Drug Delivery and Imaging. *Nat. Mater.* **2010**, *9*, 172–178.
- (9) Furukawa, H.; Cordova, K. E.; O’Keeffe, M.; Yaghi, O. M. The Chemistry and Applications of Metal-Organic Frameworks. *Science* **2013**, *341*, 123044-1–123044-12.
- (10) Deng, H.; Grunder, S.; Cordova, K. E.; Valente, C.; Furukawa, H.; Hmadeh, M.; Gándara, F.; Whalley, A. C.; Liu, Z.; Asahina, S.; et al. Large-Pore Apertures in a Series of Metal-Organic Frameworks. *Science* **2012**, *336*, 1018–1023.
- (11) Eddaoudi, M.; Kim, J.; Rosi, N.; Vodak, D.; Wachter, J.; O’Keeffe, M.; Yaghi, O. M. Systematic Design of Pore Size and Functionality in Isorecticular MOFs and Their Application in Methane Storage. *Science* **2002**, *295*, 469–472.
- (12) Furukawa, H.; Ko, N.; Go, Y. B.; Aratani, N.; Choi, S. B.; Choi, E.; Yazaydin, A. Ö.; Snurr, R. Q.; O’Keeffe, M.; Kim, J.; et al. Ultrahigh Porosity in Metal-Organic Frameworks. *Science* **2010**, *329*, 424–428.
- (13) Yaghi, O. M.; O’Keeffe, M.; Ockwig, N. W.; Chae, H. K.; Eddaoudi, M.; Kim, J. Reticular Synthesis and the Design of New Materials. *Nature* **2003**, *423*, 705–714.
- (14) Frost, H.; Snurr, R. Q. Design Requirements for Metal-Organic Frameworks as Hydrogen Storage Materials. *J. Phys. Chem. C* **2007**, *111*, 18794–18803.
- (15) Wilmer, C. E.; Leaf, M.; Lee, C. Y.; Farha, O. K.; Hauser, B. G.; Hupp, J. T.; Snurr, R. Q. Large-Scale Screening of Hypothetical Metal–Organic Frameworks. *Nature Chem.* **2012**, *4*, 83–89.
- (16) Zhang, W.; Xiong, R.-G. Ferroelectric Metal–Organic Frameworks. *Chem. Rev.* **2012**, *112*, 1163–1195.
- (17) Cui, Y.; Yue, Y.; Qian, G.; Chen, B. Luminescent Functional Metal–Organic Frameworks. *Chem. Rev.* **2012**, *112*, 1126–1162.
- (18) Allendorf, M. D.; Schwartzberg, A.; Stavila, V.; Talin, A. A. A Roadmap to Implementing Metal–Organic Frameworks in Electronic Devices: Challenges and Critical Directions. *Chem.—Eur. J.* **2011**, *17*, 11372–11388.
- (19) Silva, C. G.; Corma, A.; Garcia, H. Metal-Organic Frameworks as Semiconductors. *J. Mater. Chem.* **2010**, *20*, 3141–3156.
- (20) Li, Y.; Pang, A.; Wang, C.; Wei, M. Metal-Organic Frameworks: Promising Materials for Improving the Open Circuit Voltage of Dye-Sensitized Solar Cells. *J. Mater. Chem.* **2011**, *21*, 17259–17264.
- (21) Yang, L.-M.; Vajeeston, P.; Ravindran, P.; Fjellvåg, H.; Tilset, M. Theoretical Investigations on the Chemical Bonding, Electronic Structure, and Optical Properties of the Metal–Organic Framework MOF-5. *Inorg. Chem.* **2010**, *49*, 10283–10290.
- (22) Lin, C.-K.; Zhao, D.; Gao, W.-Y.; Yang, Z.; Ye, J.; Xu, T.; Ge, Q.; Ma, S.; Liu, D.-J. Tunability of Band Gaps in Metal–Organic Frameworks. *Inorg. Chem.* **2012**, *51*, 9039–9044.
- (23) Choi, J. H.; Choi, Y. J.; Lee, J. W.; Shin, W. H.; Kang, J. K. Tunability of Electronic Band Gaps from Semiconducting to Metallic States Via Tailoring Zn Ions in MOFs with Co Ions. *Phys. Chem. Chem. Phys.* **2009**, *11*, 628–631.
- (24) Corey, E. J. Robert Robinson Lecture. Retrosynthetic Thinking—Essentials and Examples. *Chem. Soc. Rev.* **1988**, *17*, 111–133.
- (25) Kuc, A.; Enyashin, A.; Seifert, G. Metal–Organic Frameworks: Structural, Energetic, Electronic, and Mechanical Properties. *J. Phys. Chem. B* **2007**, *111*, 8179–8186.
- (26) Alvaro, M.; Carbonell, E.; Ferrer, B.; Llabrés i Xamena, F. X.; Garcia, H. Semiconductor Behavior of a Metal-Organic Framework (MOF). *Chem.—Eur. J.* **2007**, *13*, 5106–5112.
- (27) Odbadrakh, K.; Lewis, J. P.; Nicholson, D. M. Interaction of the Explosive Molecules RDX and TATP with IRMOF-8. *J. Phys. Chem. C* **2010**, *114*, 7535–7540.
- (28) Yang, L.-M.; Ravindran, P.; Vajeeston, P.; Tilset, M. Ab Initio Investigations on the Crystal Structure, Formation Enthalpy, Electronic Structure, Chemical Bonding, and Optical Properties of Experimentally Synthesized Isorecticular Metal-Organic Framework-10 and Its Analogues: M-IRMOF-10 (M = Zn, Cd, Be, Mg, Ca, Sr and Ba). *RSC Adv.* **2012**, *2*, 1618–1631.
- (29) Yang, L.-M.; Ravindran, P.; Vajeeston, P.; Tilset, M. Properties of IRMOF-14 and Its Analogues M-IRMOF-14 (M = Cd, Alkaline Earth Metals): Electronic Structure, Structural Stability, Chemical Bonding, and Optical Properties. *Phys. Chem. Chem. Phys.* **2012**, *14*, 4713–4723.
- (30) Perdew, J. P.; Burke, K.; Ernzerhof, M. Generalized Gradient Approximation Made Simple. *Phys. Rev. Lett.* **1996**, *77*, 3865–3868.
- (31) Civalleri, B.; Napoli, F.; Noel, Y.; Roetti, C.; Dovesti, R. Ab-Initio Prediction of Materials Properties with Crystal: MOF-5 as a Case Study. *CrystEngComm* **2006**, *8*, 364–371.
- (32) Schautz, F.; Flad, H. J.; Dolg, M. Quantum Monte Carlo Study of Be₂ and Group 12 Dimers M₂ (M = Zn, Cd, Hg). *Theor. Chem. Acc.* **1998**, *99*, 231–240.
- (33) Doll, K.; Stoll, H. Ground-State Properties of Heavy Alkali Halides. *Phys. Rev. B* **1998**, *57*, 4327–4331.
- (34) Frisch, M. J.; Trucks, G. W.; Schlegel, H. B.; Scuseria, G. E.; Robb, M. A.; Cheeseman, J. R.; Scalmani, G.; Barone, V.; Mennucci, B.; Petersson, G. A.; Nakatsuji, H.; Caricato, M.; Li, X.; Hratchian, H. P.; Izmaylov, A. F.; Bloino, J.; Zheng, G.; Sonnenberg, J. L.; Hada, M.; Ehara, M.; Toyota, K.; Fukuda, R.; Hasegawa, J.; Ishida, M.; Nakajima, T.; Honda, Y.; Kitao, O.; Nakai, H.; Vreven, T.; Montgomery, J. A., Jr.; Peralta, J. E.; Ogliaro, F.; Bearpark, M.; Heyd, J. J.; Brothers, E.; Kudin, K. N.; Staroverov, V. N.; Kobayashi, R.; Normand, J.; Raghavachari, K.; Rendell, A.; Burant, J. C.; Iyengar, S. S.; Tomasi, J.; Cossi, M.; Rega, N.; Millam, J. M.; Klene, M.; Knox, J. E.; Cross, J. B.; Bakken, V.; Adamo, C.; Jaramillo, J.; Gomperts, R.; Stratmann, R. E.; Yazyev, O.; Austin, A. J.; Cammi, R.; Pomelli, C.; Ochterski, J. W.; Martin, R. L.; Morokuma, K.; Zakrzewski, V. G.; Voth, G. A.; Salvador, P.; Dannenberg, J. J.; Dapprich, S.; Daniels, A. D.; Farkas, O.; Foresman, J. B.; Ortiz, J. V.; Cioslowski, J.; Fox, D. J. *Gaussian 09*; Gaussian, Inc.: Wallingford, CT, 2009.
- (35) Meek, S. T.; Perry, J. J.; Teich-McGoldrick, S. L.; Greathouse, J. A.; Allendorf, M. D. Complete Series of Monohalogenated Isorecticular Metal–Organic Frameworks: Synthesis and the Importance of Activation Method. *Cryst. Growth Des.* **2011**, *11*, 4309–4312.
- (36) Rowsell, J. L. C.; Yaghi, O. M. Effects of Functionalization, Catenation, and Variation of the Metal Oxide and Organic Linking Units on the Low-Pressure Hydrogen Adsorption Properties of Metal–Organic Frameworks. *J. Am. Chem. Soc.* **2006**, *128*, 1304–1315.
- (37) Li, H.; Eddaoudi, M.; O’Keeffe, M.; Yaghi, O. M. Design and Synthesis of an Exceptionally Stable and Highly Porous Metal-Organic Framework. *Nature* **1999**, *402*, 276–279.
- (38) Shishkin, M.; Kresse, G. Self-Consistent GW Calculations for Semiconductors and Insulators. *Phys. Rev. B* **2007**, *75*, 235102.
- (39) Kohn, W.; Sham, L. J. Self-Consistent Equations Including Exchange and Correlation Effects. *Phys. Rev.* **1965**, *140*, A1133–A1138.
- (40) Ji, M.; Lan, X.; Han, Z.; Hao, C.; Qiu, J. Luminescent Properties of Metal–Organic Framework MOF-5: Relativistic Time-Dependent Density Functional Theory Investigations. *Inorg. Chem.* **2012**, *51*, 12389–12394.
- (41) McMurry, J. E., *Organic Chemistry* 8th ed.; Brooks/Cole: Belmont, CA, 2011.
- (42) Bally, T.; Chai, S.; Neuenschwander, M.; Zhu, Z. Pentallene: Formation, Electronic, and Vibrational Structure. *J. Am. Chem. Soc.* **1997**, *119*, 1869–1875.

(43) Tranchemontagne, D. J.; Mendoza-Cortes, J. L.; O'Keeffe, M.; Yaghi, O. M. Secondary Building Units, Nets and Bonding in the Chemistry of Metal-Organic Frameworks. *Chem. Soc. Rev.* **2009**, *38*, 1257–1283.

(44) Jaitner, P.; Rieker, C.; Wurst, K. Aggregation of Carbamate Ligands around the $[\text{Co}_4\text{O}]^{6+}$ Core. Synthesis and Structure of the Cluster $[\text{Co}_4\text{O}(\text{O}_2\text{CNC}_9\text{H}_{18})_6]$ Prepared by a Novel Oxo-Transfer Reaction of the Nitroxyl Free Radical 2,2,6,6-Tetramethylpiperidin-1-oxyl with $[\text{Co}_2(\text{CO})_8]$. *Chem. Commun.* **1997**, 1245–1246.

(45) Tulinsky, A.; Worthington, C. R.; Pignataro, F. Basic Beryllium Acetate. I. The Collection of Intensity Data. *Acta Crystallogr.* **1959**, *12*, 623–626.

(46) Ockwig, N. W.; Delgado-Friedrichs, O.; O'Keeffe, M.; Yaghi, O. M. Reticular Chemistry: Occurrence and Taxonomy of Nets and Grammar for the Design of Frameworks. *Acc. Chem. Res.* **2005**, *38*, 176–182.

(47) Wu, Y.; Chan, M. K. Y.; Ceder, G. Prediction of Semiconductor Band Edge Positions in Aqueous Environments from First Principles. *Phys. Rev. B* **2011**, *83*, 235301.